International Journal of Technology (2017) 1: 66-75
ISSN 2086-9614

PHASE TRANSITIONS IN $La_{0.73}Ca_{0.27}Mn_{1-x}Cu_xO_3$ ($0 \leq X \leq 0.19$)

Y. E. Gunanto[1*], W. A. Adi[2], B. Kurniawan[3], S. Poertadji[3], T. Ono[4], H. Tanaka[5], E. Steven[6]

[1]*Department of Biology Education, Faculty of Education, University of Pelita Harapan, Karawaci, Tangerang 15811, Indonesia*
[2]*Center for Science and Technology of Advanced Materials, BATAN, Tangerang Selatan 15314, Indonesia*
[3]*Department of Physics, University of Indonesia, Depok 16424, Indonesia*
[4]*Department of Physics, Osaka Prefecture University, Sakai, Osaka 599-8531, Japan*
[5]*Department of Physics, Tokyo Institute of Technology, Meguro-ku, Tokyo 152-8551, Japan*
[6]*Department of Physics, National High Magnetic Field Lab., Tallahassee, Florida 32310, USA*

(Received: October 2016 / Revised: January 2017 / Accepted: January 2017)

ABSTRACT

We have performed resistivity measurements as a function of temperature, with and without an external magnetic field. Magnetization measurements are also done as a function of temperature M(T) as well as a function of an external magnetic field M(H) for $La_{0.73}Ca_{0.27}Mn_{1-x}Cu_xO_3$ compounds with $0 \leq x \leq 0.19$. The samples with $x = 0$ and 0.06 are insulators. As for the samples with $x = 0.10$, 0.13, and 0.19, they undergo an insulator to metal transition as the temperature is lowered. The insulator-metal transition temperatures are 24 K, 74 K, and 69 K for $x = 0.10$, 0.13, and 0.19, respectively. The magnetoresistance decreases with increasing values of Cu, i.e. 75%, 72%, 64%, and 35% for $x = 0$, 0.06, 0.10, and 0.13 respectively. Samples in accordance with the model of crystalline metal Ln R vs. 1/T are compared to Mott insulator models Ln R vs. $1/T^{0.25}$. Based on the magnetization curve, a paramagnetic to ferromagnetic transition is observed at Curie temperature, T_C, of ~ 196 K, 170 K, 140 K, 137 K, and 113 K for $x = 0$, 0.06, 0.10, 0.13, and 0.19 respectively.

Keywords: Curie temperature; Magnetoresistance; Metal-insulator transition

1. INTRODUCTION

Manipulations of the electronic and/or magnetic properties of materials are the key to the advancement of novel devices. Multi-functional materials, where both the electronic and magnetic properties are tunable, are especially versatile for developing sensors, magnetic storage devices, and other types of devices. In the last decade, many studies have been done on the compound perovskite manganites $La_{1-x}Ca_xMnO_3$ about how the chemical doping in La-sites affects material properties (Kumar et al., 2014; Gencer et al., 2014; Jagtap et al., 2013; González-Calbet et al., 2004; Freitas et al., 2004; Pissas & Kallias, 2003).

More recently, it has been shown that chemical doping, in this case with Cu, at the Mn site significantly alters the material's resistivity, lattice parameters, crystal structure, and various transition temperatures (Kumar et al., 2011; Kim et al., 2008; El-Hagary et al., 2008; Craus & Lozovan, 2006; Kim et al., 2005). Some studies attribute such changes to the modification of the Mn^{3+}-O-Mn^{4+} interaction, and the more complicated interactions

*Corresponding author's e-mail: yohanes.gunanto@uph.edu, Tel.: +62-021-546-6057; fax: +62-021-546-1055
Permalink/DOI: https://doi.org/10.14716/ijtech.v8i1.5980

between the center Mn ions and the dopant Cu ions (Kumar et al., 2011) that are in a mixed state between Cu^{2+} and Cu^{3+}, with Cu^{2+} being more dominant (Kim et al., 2008; Kim et al., 2005). Another study, however, suggests that for lower values of Cu-doping (x = 0-0.2), the Cu ions are in a Cu^{2+} state with a rhombohedral crystal structure, whereas for Cu-doping of 0.3-0.5, orthorhombic Cu^{3+} ions are formed (El-Hagary et al., 2008). In spite of these results, a deeper understanding on how Cu-doping affects physical properties is still unclear.

In this paper, we discuss the interplays between the Mn-Cu ions in $La_{0.73}Ca_{0.27}Mn_{1-x}Cu_xO_3$ (with $0 \leq x \leq 0.19$), and how they result in the tuning of the electronic and magnetic properties, in particular the insulator-metal and paramagnetic-ferromagnetic phase transition temperatures.

2. EXPERIMENTAL

Samples of Cu-substituted $La_{0.73}Ca_{0.27}Mn_{1-x}Cu_xO_3$ with $0 \leq x \leq 0.19$ were prepared using the conventional solid state reaction method (Gunanto et al., 2011) from materials La_2O_3, $CaCO_3$, MnO_2 and CuO with purity above 99%. High energy milling (HEM) was used to mix these materials. All samples were heated at a temperature of 1350^{o}C for 6 hours, after which they were milled again. Finally, they were kept at 1100^{o}C for 24 hours. X-Ray Diffraction (XRD) was used to characterize the crystal structure, showing the presence of a single phase with a crystal structure orthorhombic and space group Pnma of the materials. To know the magnetic structure of the samples, further characterization was carried out using High Resolution Powder Diffraction (HRPD) (λ = 1.8223 Å) at the Laboratory for Neutron Scattering BATAN, Serpong, Tangerang.

Resistance measurements at various temperatures and magnetic fields were carried out using a Physical Properties Measurement System (PPMS) in four probe configurations. Polycrystalline powders were compressed into pellets of equal thickness for each sample types. The samples were then cut to ~7 mm (length) by 3 mm (width) where 4-probe carbon paste contacts were applied at an equally spaced distance from one another to minimize the resistance variation due to the geometry of the electrodes. Magnetization measurements were done in SQUID Magnetic Properties Measurement Systems (MPMS).

3. RESULTS AND DISCUSSION

The temperature-dependent electrical resistance R of the $La_{0.73}Ca_{0.27}Mn_{1-x}Cu_xO_3$ for x = 0 (undoped sample) is shown in Figure 1. The sample exhibits good insulating behavior from room down to cryogenic temperatures (Figure 1a). For amorphous insulators, typically the transport behavior follows Mott's Variable Range Hopping model very well, where Ln $R \sim 1/T^{0.25}$ (Wang et al., 2001). However, we find that compared to the Mott model, the Arrhenius model Ln $R \sim 1/T$ (which applies to crystalline insulators) fits equally well (Figures 1b and 1c). Under external magnetic fields H (Figure 1), the overall resistance is decreased (negative magnetoresistance) but still follows similar temperature-dependent behavior as that at zero magnetic fields. The activation energies, E_a, at H = 0 T and H = 8.5 T, are found to be 8.9×10^{-6} eV and 1.3×10^{-5} eV, respectively, according to Equation 1 below,

$$R = C\, exp(E_a/kT) \tag{1}$$

where R is the electrical resistance, C is factor pre-exponential containing among others the concentration of charge-carrier, T is absolute temperature, k is the Boltzmann's constant, and E_a is the activation energy.

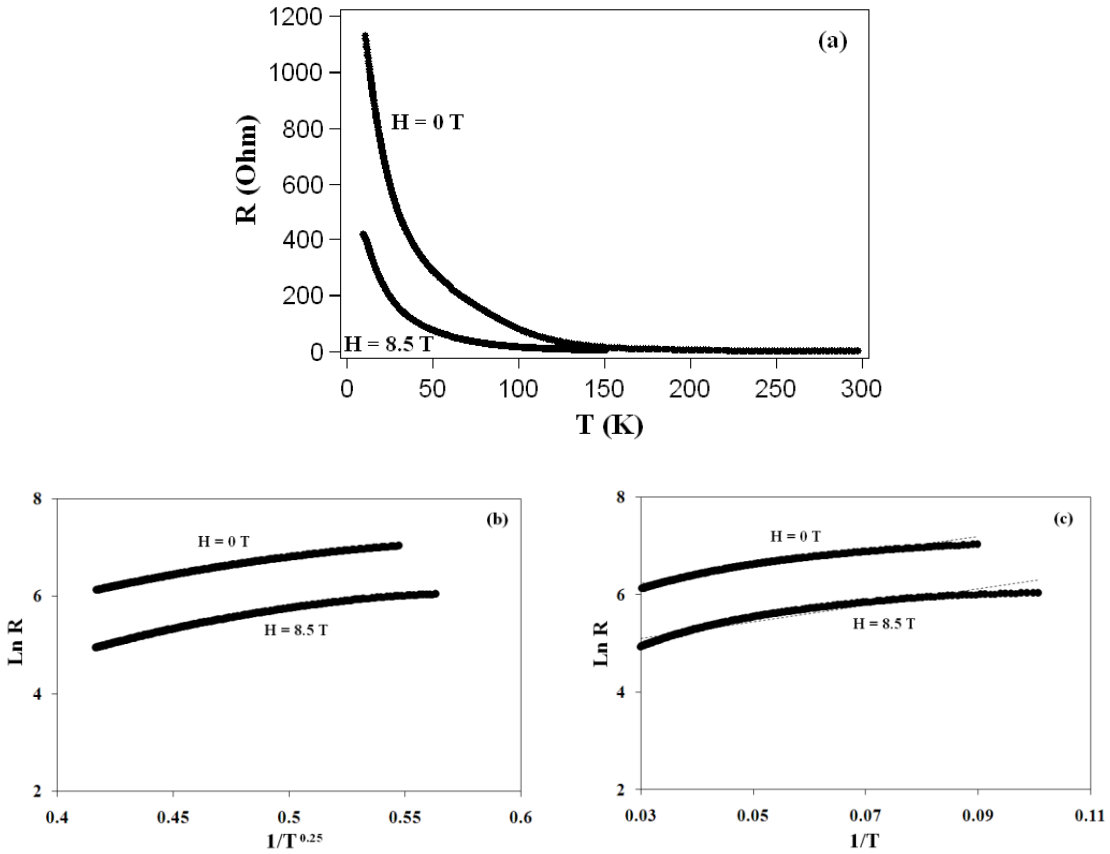

Figure 1 (a) Temperature-dependent resistance of $La_{0.73}Ca_{0.27}Mn_{1-x}Cu_xO_3$; (b) Mott model of Ln *R* as a function of $1/T^{0.25}$; and (c) Arrhenius model of Ln *R* as a function of *1/T* for $x = 0$ at 0 T and 8.5 T

Similar to the undoped samples, the Cu-doped samples (Figure 2a) are also consistent with the general transport behavior described above. More importantly, we observe three main effects of increasing the Cu concentration in the transport properties. First, the room temperature resistance increased with Cu-doping up to $x = 0.13$ and then decreases with Cu-doping of $x = 0.19$ (Figure 2b). Second, the magnetoresistance, defined as R(H) – R(H=0T) was suppressed. We found that at 145 K, the resistance decrease for samples $x = 0$, 0.06, 0.10, and 0.13 was 75%, 72%, 64%, and 35%, respectively (Figure 2b). Finally, an insulator to the metal phase transition was observed for samples with $x = 0.10$, 0.13, and 0.19 with transition temperatures T_{IM} of 24 K, 74 K, and 69 K, respectively (Figure 3).

To understand these effects, it is important to first note that the Cu ions can exist in two states at different sizes, Cu^{2+} (~0.73 Å) and Cu^{3+} (~0.54 Å) (Shannon, 1976). Likewise, the Mn ions can exist in two states, Mn^{3+} (~0.645Å) and Mn^{4+}, as a result of the trivalent La^{3+} ions being replaced by the divalent Ca^{2+} ions, which introduced holes on the Mn sites.

At lower Cu-doping concentrations, the Cu^{2+} ions which are larger than the Mn^{3+} are dominant, inducing internal chemical pressure (Kumar et al., 2011) that lowers the resistance of the sample. In contrast, at higher Cu-doping, the smaller Cu^{3+} ions are dominant, therefore reducing the internal chemical pressure, effectively increasing the resistance. Also, the Cu-doping can reduce the Mn^{3+} ($3d^4$, t_{2g}^3-e_g^1) - Mn^{4+} ($3d^3$, t_{2g}^3-e_g^0) ratio, therefore reducing the double exchange interaction, and hopping electrons and sites (Kim et al., 2005).

With changes in the valence of the ions, the ionic radius changes; this does not only change the crystal structure, but also changes the magnetic properties and charge localization (El-Hagary, et al., 2008; Craus & Lozovan, 2006; Szytula, 2010). As discussed by El-Hagary et al. (2008)

increasing the Cu concentration localizes and decreases the mobility of e_g electrons of Mn^{3+}. The suppression of the magnetoresistance can therefore be attributed to the higher energy (and therefore external magnetic fields) required to delocalize the electrons in higher Cu-doped samples.

Finally, the variation in T_{IM} with the amount of added Cu is explained on the basis of the double exchange mechanism. The Cu substitutions have been found to perturb the Mn^{3+}-O-Mn^{4+} network and have influence on T_{IM}. The effect of Cu substitution on the Mn position can change the order of the orbital Mn^{3+} ions, as well as weaken the double exchange between Mn^{3+} and Mn^{4+}. Similar results were also obtained by Kumar et al. (2011).

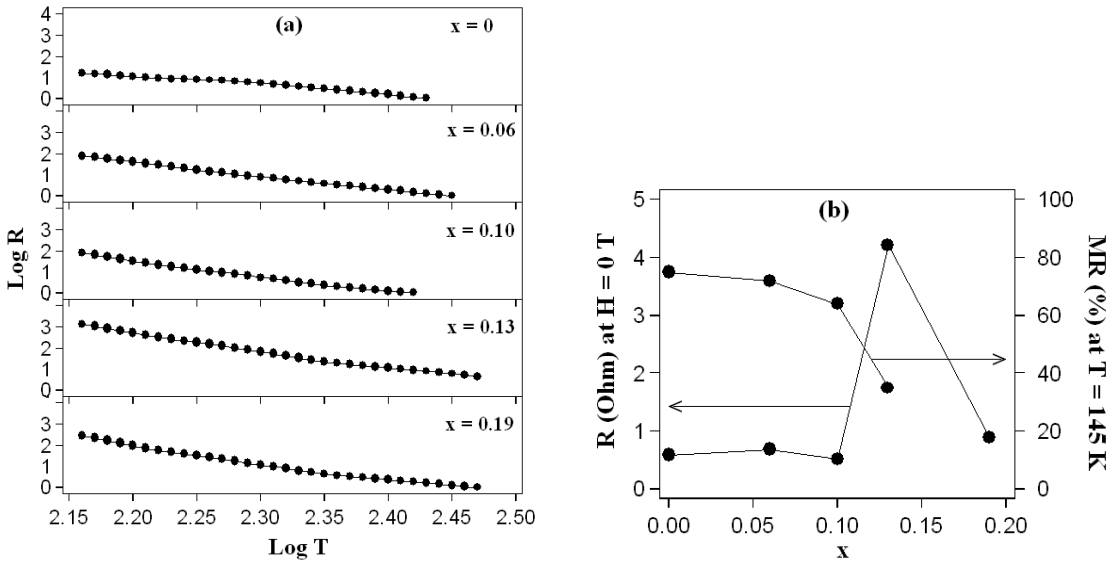

Figure 2 (a) Temperature-dependent resistance of $La_{0.73}Ca_{0.27}Mn_{1-x}Cu_xO_3$ at 145 K – 300 K; and (b) Room temperature resistance (left axis) vs Cu concentration and magnetoresistance (right axis) vs concentration

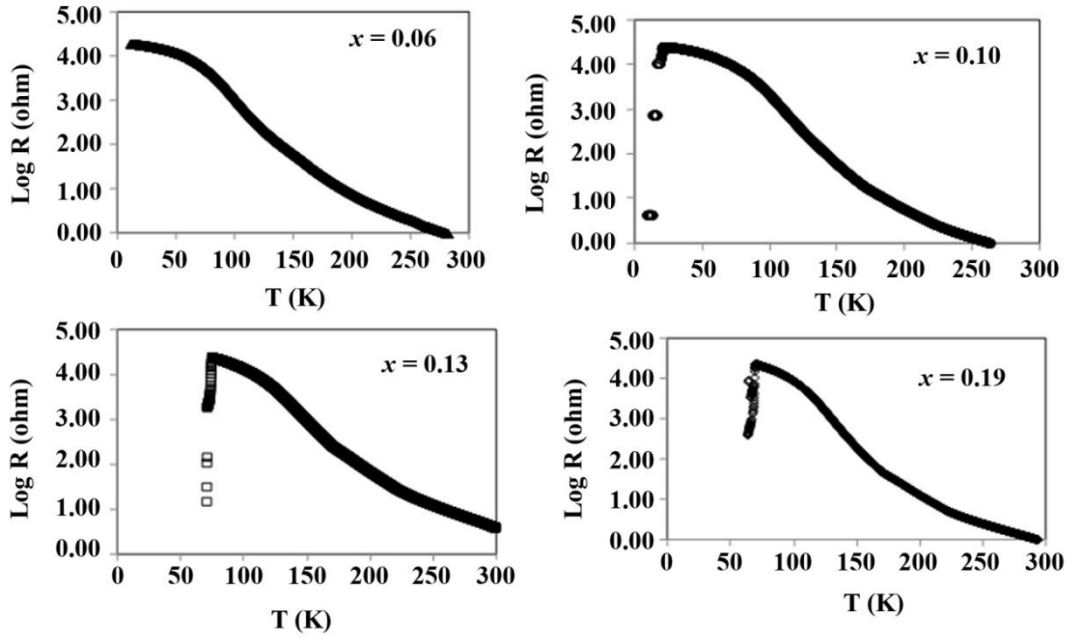

Figure 3 Resistivity as a function of temperature of $La_{0.73}Ca_{0.27}Mn_{1-x}Cu_xO_3$ for x = 0.06, 0.10, 0.13, and 0.19

With regard to the effects of increasing the Cu concentrations in the magnetic properties, our neutron scattering (Kim et al., 2005; Gunanto et al., 2012a; Gunanto, et al., 2013) and SQUID measurements revealed that all samples were orthorhombic both at room and low temperatures, whereas the magnetic structure at room temperature was paramagnetic and ferromagnetic at low temperatures (Figure 4).

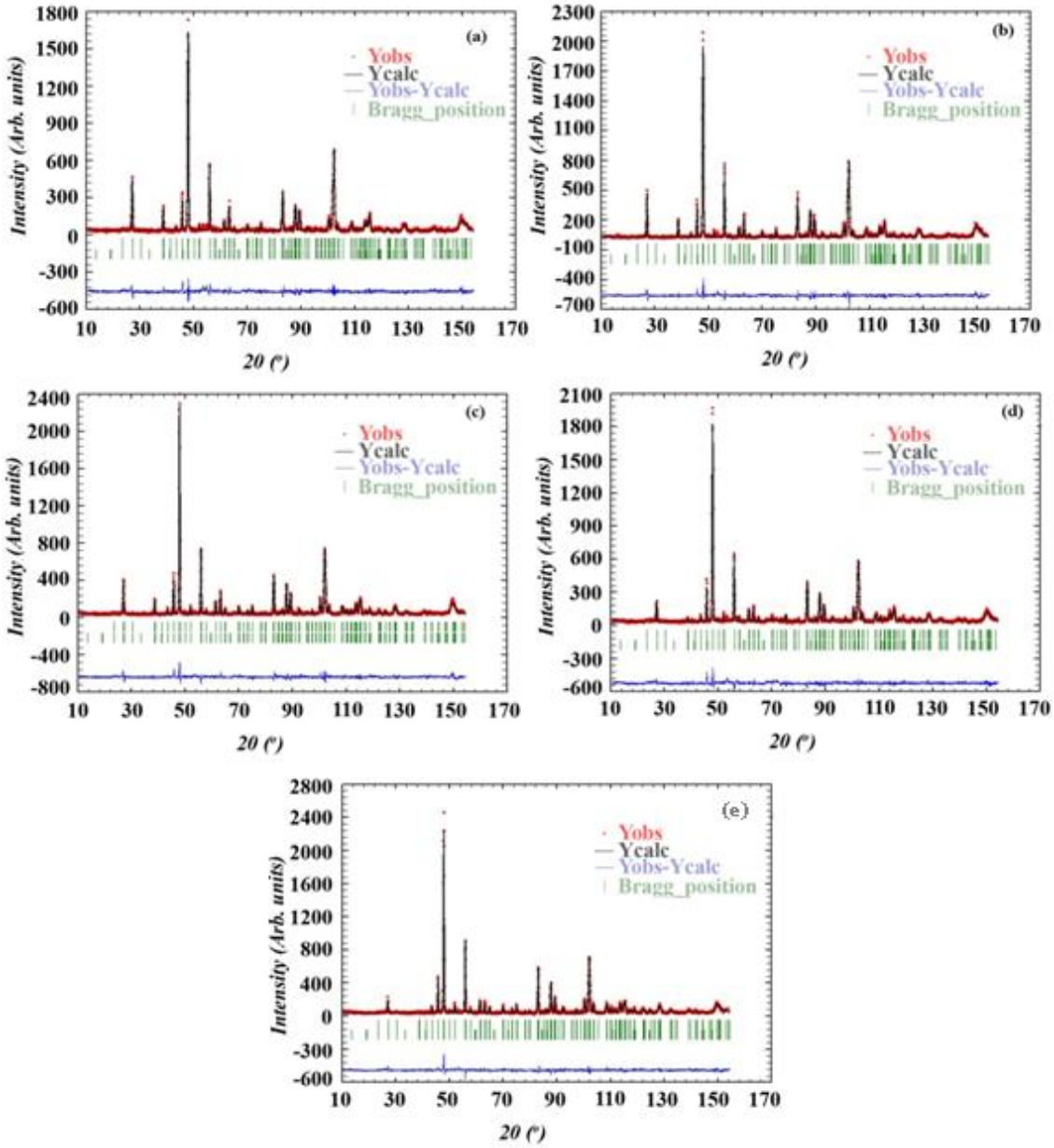

Figure 4 Diffraction patterns from neutron scattering a low temperature (a)- (e) for *x*=0-0.19, respectively

The particle morphology of SEM photograph is shown in Figure 5. The image morphology of particles shows that the particle shapes at the various particle sizes and uniform and homogenous on the surface of the sample. Figure 6 shows the four possible magnetic structures for propagation vector **q** = (0,0,0) (Gunanto et al., 2011). Lattice parameters are shown in Table 2. The temperature dependent of the magnetization measurement, M(T) in both zero-field cooling (ZFC) and field-cooling (FC) of $La_{0.73}Ca_{0.27}Mn_{1-x}Cu_xO_3$ ($0 \leq x \leq 0.19$) at 20 Oe is

presented in Figures 6a- 6d. A drastic change in M around the Curie temperature T_C indicates magnetic ordering from a paramagnetic (PM) to ferromagnetic phase (FM). For x = 0 (Figure 7a), at 197 K, the magnetization starts to rise rapidly with decreasing temperature. A clear transition at 197 K can also be seen in 1/susceptibility vs temperature curve in Figure 7f. Below 197 K, the ZFC and FC magnetization are separated from each another. This confirms that the onset of the FM order in the sample occurs at a temperature of 197 K. Detailed results can be seen in the Table 1.

It is clear that the substitution of Cu on the Mn site will cause a reduction in the Curie temperature, T_C. Of note, the lowering of T_C is in contrast to how the T_{IM} is increased by the Cu-doping. Previous studies have found that would reduce the value of the magnetic moment (Gunanto et al., 2012b; Gunanto et al., 2013). We agree with the explanation by El-Hagary et al. (2008), that this is caused by a decrease in the mobility of e_g electrons of Mn^{3+} and they become more localized (El-Hagary et al., 2008); therefore, the double exchange interaction is weakened by the increase in Cu-doping.

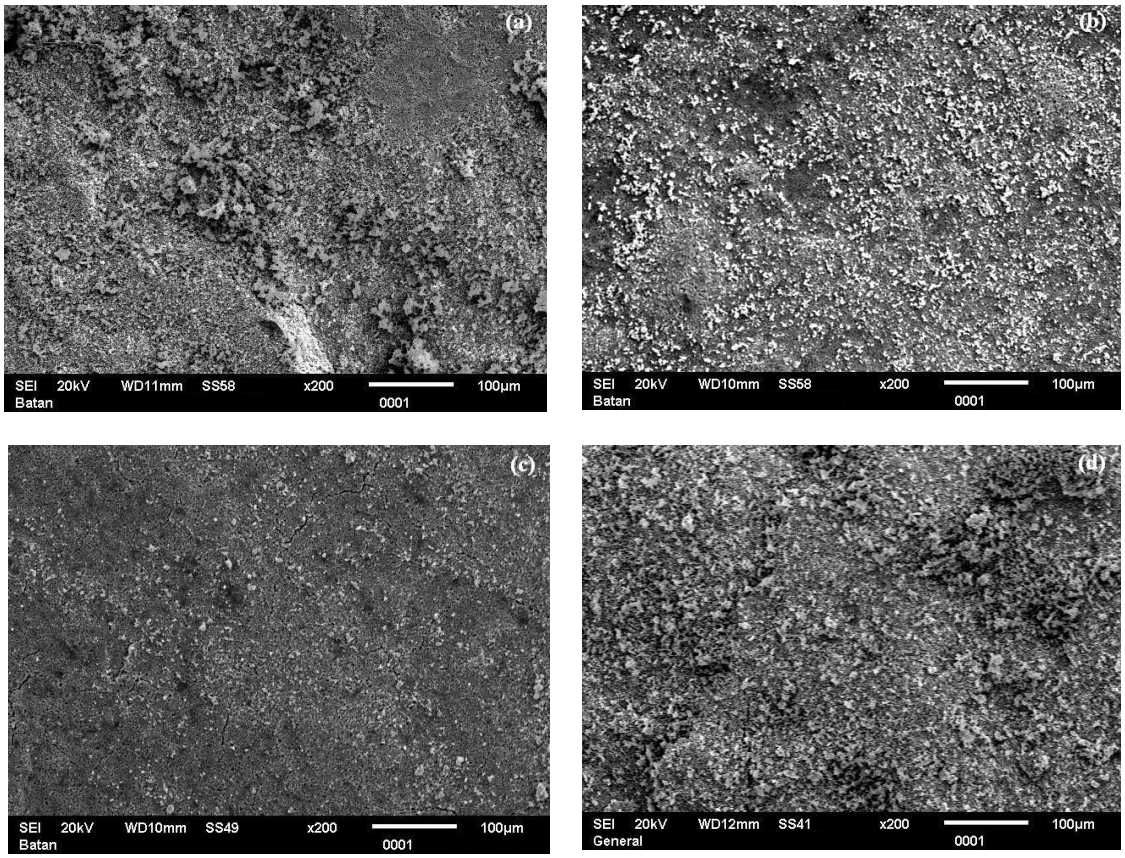

Figure 5 The particle morphology of the samples (a)- (d) for *x* = 0.06, 0.10, 0.13, and 0.19, respectively

Table 1 The curie temperature T_C for $La_{0.73}Ca_{0.27}Mn_{1-x}Cu_xO_3$ ($0 \leq x \leq 0.19$)

x	T_C (K)
0	197
0.06	170
0.10	140
0.13	137
0.19	113

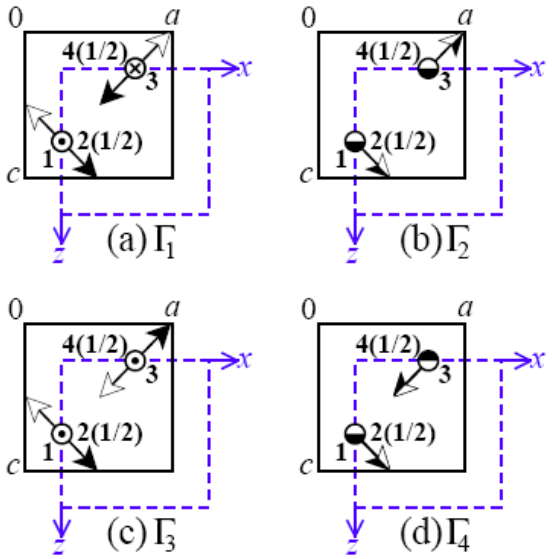

Figure 6 Four possible magnetic structures for $\boldsymbol{q}$ = (0,0,0): (a) Γ_1; (b) Γ_2; (c) Γ_3; and (d) Γ_4. Boxes with solid lines are the shifted crystallographic unit cells containing 4 atoms. The atom positions are based on the coordinate axis with dashed lines. Numbers in brackets denote the fractional *y*-coordinates of the respective atoms: Mn_1 (0,0,½) Mn_2 (0,½,½) Mn_3 (½,0,0) and Mn_4 (½,½,0)

Table 2 Lattice parameters for $La_{0.73}Ca_{0.27}Mn_{1-x}Cu_xO_3$ ($0 \leq x \leq 0.19$)

Sample	Lattice parameters at room temperature			
	a (Å)	*b* (Å)	*c* (Å)	χ^2
Cu = 0.00	5.4847(2)	7.7603(3)	5.5202(2)	1.36
Cu = 0.06	5.4842(2)	7.7615(3)	5.5196(2)	1.28
Cu = 0.10	5.4943(2)	7.7762(2)	5.5203(1)	1.53
Cu = 0.13	5.4835(3)	7.7582(4)	5.5106(2)	1.75
Cu = 0.19	5.4916(2)	7.7700(3)	5.5166(2)	1.85

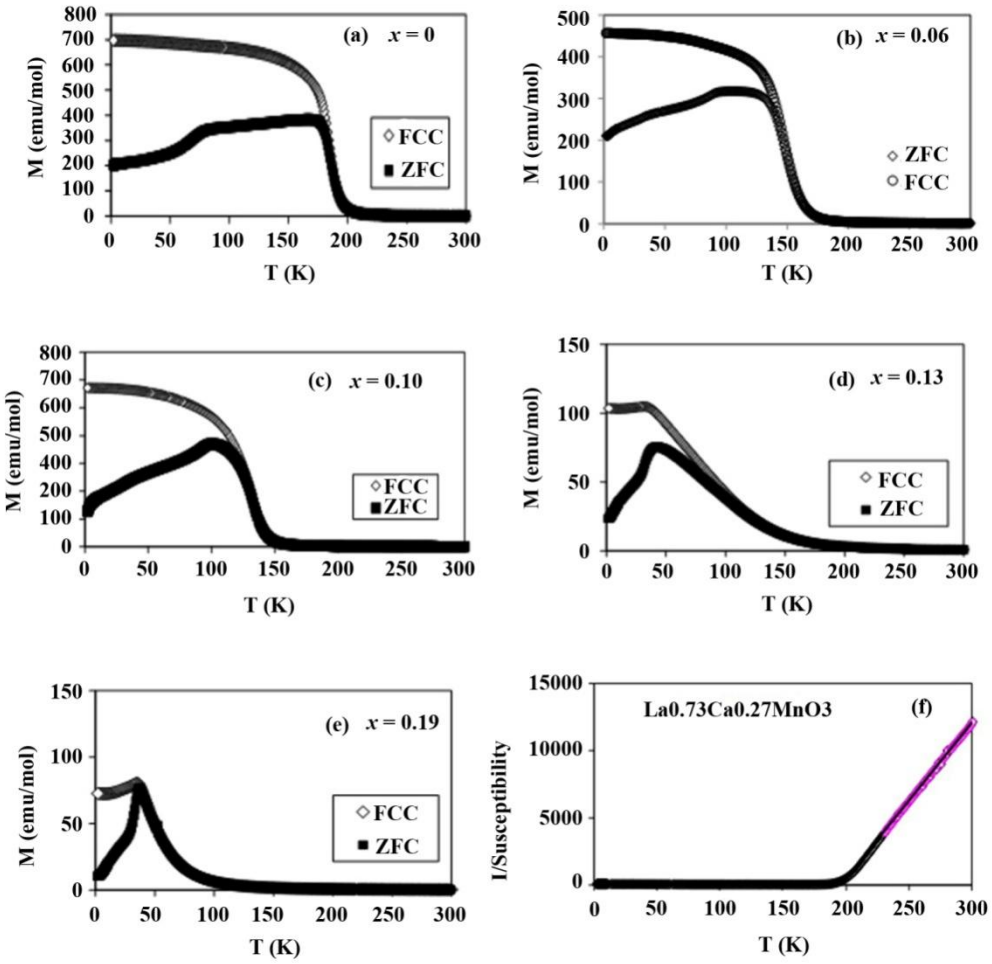

Figure 7 (a- e) The zero-field cooling (ZFC) and field-cooling (FC) magnetization of $La_{0.73}Ca_{0.27}Mn_{1-x}Cu_xO_3$ as a function of temperature, measured in 20 Oe for x = 0, 0.06, 0.10, 0.13 and 0.19; and (f) 1/susceptibility as a function of temperature for x = 0

4. CONCLUSION

We have shown that both the electronic and magnetic properties can simultaneously be tuned by Cu substitution at Mn sites in $La_{0.73}Ca_{0.27}Mn_{1-x}Cu_xO_3$ ($0 \leq x \leq 0.19$). Increasing the Cu concentration promotes the insulator-metal but suppresses the paramagnetic-ferromagnetic phase transitions in the materials. Samples with x=0 and 0.06 are insulators, and samples with x = 0.10, 0.13, and 0.19 exhibit insulator-metal transition at 24 K, 74 K, and 69 K, respectively. The paramagnetic-ferromagnetic transition temperatures are 196 K, 170 K, 140 K, 137 K, and 113 K for x = 0, 0.06, 0.10, 0.13, and 0.19, respectively. Both phenomena are evaluated based on the interplay between the various states of Cu and Mn ions at lower and higher concentrations, where the Cu ions reduce the chemical pressure, localize the e_g electron, and weaken the double exchange interactions between the Mn ion networks.

5. ACKNOWLEDGMENT

We are grateful for the support and facilities provided by BATAN (Indonesian Nuclear Energy Agency), and the Tanaka Lab. for Low Temperature, Tokyo Institute of Technology Japan. A portion of this work was carried out at the National High Magnetic Field Laboratory.

6. REFERENCES

Craus, M.-L., Lozovan, M., 2006. Structure and Magnetoresistance of $La_{1-x}Ca_xMn_{0.9}Cu_{0.1}O_3$ Manganites. *J. Optoelectronic and Advanced Materials,* Volume 8(3), pp. 1008- 1011

El-Hagary, M., Shoker, Y.A., Mohammad, S., Moustafa, A.M., Abd. El-Aal, A., Michor, H., Reissner, M., Hilscher, G., Ramadan, A.A., 2008. Structural and Magnetic Properties of Polycrystalline $La_{0.77}Sr_{0.23}Mn_{1-x}Cu_xO_3$ ($0 \leq x \leq 0.3$) Manganites. *Journal Alloys and Compound*, pp. 1- 7

Freitas, R.S., Ghivelder, L., Sacanell, J., Levy, P., Parisi, F., 2004. Magnetoresistance in Phase-separated $La_{0.5}Ca_{0.5}MnO_3$ Manganite. *Journal of Magnetism and Magnetic Materials*, Volume 272-276, pp. 1745- 1747

Gencer, H., Cengiz, N.E., Kolat, V.S., Izgi, T., Atalay, A., 2014. Production of $LaCaMnO_3$ Composite by Ball Milling. *Acta Physica Polonica A*, Volume 125, pp. 214- 216

González-Calbet, J.M., Alonso, J.M., Arroyo, A., Cortés-Gil, R., Multigner, M., Hernando, A., Vallet-Regí, M., 2004. Ferro-antiferromagnetic Transition in Slightly Doped Manganites. *Solid State Ionics,* Volume 172, pp. 549- 551

Gunanto, Y.E., Purwanto, A., Kurniawan, B., Poertadji, S., Fajar, A., Mugirahardjo, H., Wisnu, A.A., 2011. The Influence of Cu-doping on the Structural and Magnetic Properties of $La_{0.73}Ca_{0.27}Mn_{1-x}Cu_xO_3$ ($0 \leq x \leq 0.19$). *In:* Proceedings of the 4th Nanoscience and Nanotechnology Symposium, AIP Conference Proceeding. Volume 1415, pp. 148- 151

Gunanto, Y.E., Purwanto, A., Andika, F., Mugirahardjo, H., Wisnu, A.A., Kurniawan, B., Poertadji, S., 2012a. The Use of High Resolution Powder Diffraction to Determine Crystal Structure and Magnetic on Compound $La_{0,47}Ca_{0,53}Mn_{1-Y}Cu_yO_3$ ($0 < y < 0,09$). *Indonesian Journal of Materials Science*, Volume 14(1), pp. 8- 12

Gunanto, Y.E., Kurniawan, B., Purwanto, A., Wisnu, A.A., Poertadji, S., 2013. The Effect of Cu Doping on Crystal Structure and Magnetoresistance in $La_{0.73}Ca_{0.27}Mn_{1-x}Cu_xO_3$ with $0 \leq x \leq 0.19$. *Indonesian Journal of Materials Science*, Volume 14(3), pp. 199- 202

Gunanto, Y.E., Kurniawan, B., Poertadji, S., Wisnu, A.A., Purwanto, A., Tanaka, H., Ono, T., 2012b. The Structural and Magnetic Properties of $La_{1-x}Ca_xMnO_3$ with $x = 0.27$ and 0.47. *Indonesian Journal of Materials Science*, Volume 13(3), pp. 188- 191

Jagtap, P.P., Chaudhari, Y.A., Abuassaj, E.M., Patil, P.B., Bendre, S.T., 2013. Structural, Electrical and Magnetotransport Properties of $La_{0.7}Ca_{0.2}Sr_{0.1}MnO_3$ by Self Propagating High Temperature Synthesis. *IOSR Journal of Applied Physics (IOSR-JAP)*, Volume 5(3), pp. 64- 68

Kim, M.S., Yang, J. B., Medvedeva, J., Yelon, W.B., Parris, P.E., James, W.J., 2008. Electronic Structure of $La_{0.7}Sr_{0.3}Mn_{1-x}Cu_xO_3$ ($0.0 \leq x \leq 0.30$). *Journal of Physics: Condensed. Matter*, Volume 20(25), pp. 1- 7

Kim, M.S., Yang, J.B., Paris, P.E., Cai, Q., Zhou, X.D., James, W.J., Yelon, W.B., Buddhikot, D., Malik, S.K., 2005. The Effect of Cu-doping on the Magnetic and Transport Properties of $La_{0.7}Sr_{0.3}MnO_3$. *Journal Applied Physics*, Volume 97, pp. 1- 3

Kumar, P.A., Mathieu, R., Nordblad, P., Ray, S., Karis, O., Andersson, G., Sarma, D.D., 2014. Reentrant Superspin Glass Phase in $La_{0.82}Ca_{0.18}MnO_3$ Ferromagnetic Insulator. *Physical Review X*, Volume 4, 011037-1- 011037-7

Kumar, P., Dwivedi, R.K., Ravikant, P., Praveen, K.S., Singh, H.K., 2011. Magneto-transport Properties of $La_{0.80}Sr_{0.20}Mn_{1-x}Cu_xO_3$ Thin Films Fabricated by using Spray Pyrolysis. *Journal the Korean Physical Society*, Volume 58(1), pp. 58- 63

Panopoulus, N., Koumoulis, D., Diamantopoulos, G., Belesi, M., Fardis, M., Pissas, M., Papavassiliou, G., 2010. Spin Order and Lattice Frustration in Optimally Doped Manganites: A High-temperature NMR Study. *Physical Review B*, Volume 82, pp. 1- 8

Pissas, M., Kallias, G., 2003. Phase Diagram of the $La_{1-x}Ca_xMnO_3$ compound ($0.5 \leq x \leq 0.9$). *Physical Review B*, Volume 68(13), pp. 1- 9

Shannon, R.D., 1976. Revised Effective Ionic Radii and Systematic Studies of Interatomic Distance in Halides and Chalcogenides. *Acta Crystallographica Section A*, Volume A32, pp. 751- 767

Szytula, A., 2010. Manganites Structural Aspects. *Acta Physica Polonica A*, Volume 118(2), pp. 303- 306

Wang, K.Y., Song, W.H., Dai, J.M., Ye, S.L., Wang, S.G., Sun, Y.P., Du, J.J., 2001. The Influence of Cu Doping on the Charge-ordering of $La_{0.5}Ca_{0.5}MnO_3$. *Journal Physica Status Solidi (A)*, Volume 184(2), pp. 515- 522